Mapping an Almond Bar wedge at Stagecoach Draw Field, southwestern Wyoming:

Application of spectral decomposition technique

Yuriy Ganshin, Scott A. Quillinan, Ronald C. Surdam

WSGS

Wyoming State Geological Survey

Report of Investigations No. 59

2010

WSGS

Director and State Geologist Ronald C. Surdam

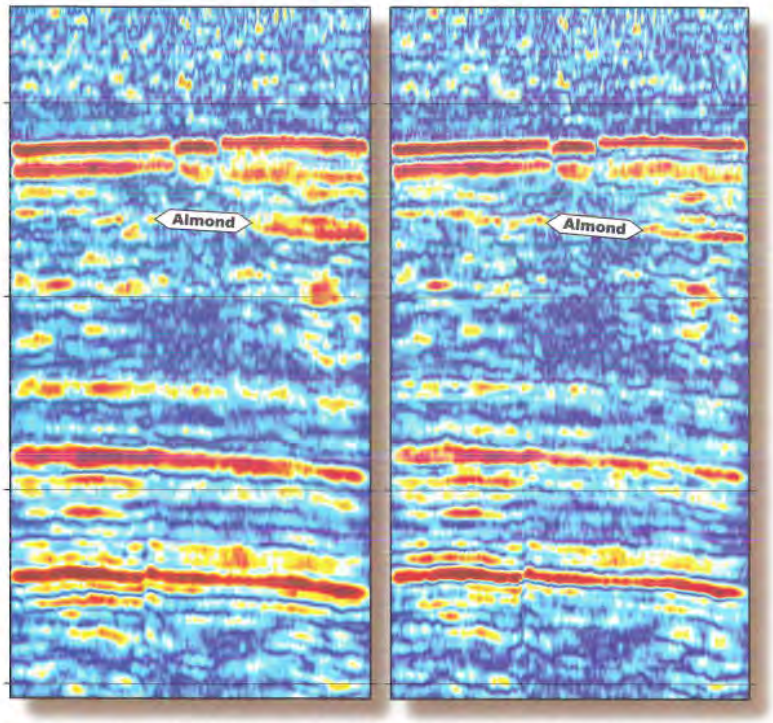

Northeast–southwest isofrequency sections from the spectrally decomposed 3-D seismic volume across Stagecoach Draw Field. From Figure 11 (p. 15).

Edited by:
Robert W. Waggener
Tamara T. Linse

Design by:
Brendon B. Orr
Robert W. Waggener

Layout by:
Brendon B. Orr

First printing of 500 copies by Printco Graphics Inc., June 2010.

Mapping an Almond Bar wedge at Stagecoach Draw Field, southwestern Wyoming: Application of spectral decomposition technique, by Yuriy Ganshin, Scott A. Quillinan, and Ronald C. Surdam with contributions from others. Seismic data provided by WesternGeco, but the interpretation of the data is that of the authors.

Wyoming State Geological Survey (WSGS) Report of Investigations No. 59, 2010.
ISBN 978-1-884589-52-2

Copyright © 2010 by the WSGS. All rights reserved.

The WSGS encourages the fair use of its material. We request that credit be expressly given to the "Wyoming State Geological Survey" when citing information from this publication. Please contact the WSGS at 307-766-2286, ext. 224, or by e-mail at sales-wsgs@uwyo.edu if you have any questions about citing materials, preparing acknowledgments, or extensive use of this material. We appreciate your cooperation.

Any use of trade, product, or firm names in this publication is for descriptive purposes only and does not imply endorsement or approval by the State of Wyoming or the WSGS. Individuals with disabilities who require an alternative form of this publication should contact the WSGS (see contact information above). TTY relay operator 800-877-9975.

For more information about the WSGS or to order publications and maps, please go to www.wsgs.uwyo.edu, call 307-766-2286, ext. 224, or e-mail sales-wsgs@uwyo.edu.

Cover: Upper Almond outcrop on the Rock Springs Uplift, southwestern Wyoming. *Photo by Alan J. Ver Ploeg, WSGS.*

Mapping an Almond Bar wedge at Stagecoach Draw Field, southwestern Wyoming:

Application of spectral decomposition technique

Wyoming State Geological Survey
Report of Investigations No. 59
2010

Yuriy Ganshin, Scott A. Quillinan, Ronald C. Surdam

Seismic data provided by WesternGeco. Interpretation of the data is that of the authors.

Table of Contents

Abstract....1
Introduction....1
Geological Setting....1
Seismic and Log Data....3
Method....5
Wedge Modeling....7
Delineation of the Almond Reservoir Sandstone....13
Conclusions....18
Acknowledgments....19
References Cited....19

Abstract

Thinning, pinched-out beds of the Cretaceous Almond Formation and potential areas for gas exploration are defined using a seismic spectral decomposition technique. The principal gas production at Stagecoach Draw comes from the uppermost sandstone in the Almond Formation, a marginal marine deposit that thins and becomes nonmarine west of the field. Current field development, consisting of approximately 30 wells, has proven that both structural and stratigraphic hydrocarbon trapping occurs at approximately a depth of 8,000 feet along the crest of the southeasterly plunging Sandy Bend Arch. A 3-D seismic survey covering approximately 85 square miles was acquired in 1996 to facilitate field exploitation.

This report presents both structural and stratigraphic interpretations of the seismic data set after it was reprocessed using time-frequency analysis of seismic reflection signals. The extent of the Almond pay sandstones has been mapped in more detail utilizing spectral decomposition techniques. Reservoir and non-reservoir facies were differentiated by comprehensive, integrated seismic attribute analysis. The integrated work combined 3-D seismic data with gamma-ray logs from 36 wells. A strong correlation between seismic frequency content and thickness gradient is shown. The spectral decomposition method is a valuable aid in enhancing the ability to map thin beds in the tight gas sandstone environments of the Rocky Mountain region. Results from this study are important for the reservoir modeling and site characterization phases of Stagecoach Draw Field development and expansion. Most importantly, it shows that seismic time-frequency analysis significantly assists in delineating gas-saturated reservoir rocks. Lastly, this study identifies a large area southeast of Stagecoach Draw that demonstrates similar seismic attributes to reservoir rocks at the Stagecoach Draw Field.

Introduction

The principal gas production at Stagecoach Draw comes from a combination of structural and stratigraphic traps in the upper Almond marginal marine sandstone. This sequence thins and becomes a nonmarine deposit west of the field. Current field development includes approximately 30 wells that primarily produce gas at a depth of about 8,000 feet along the crest of the southeasterly plunging Sandy Bend Arch. An 85-square-mile 3-D seismic survey was run in 1996 to facilitate field exploitation. Conventional processing and analysis of the 3-D data resulted in structural maps of the Almond production interval (Kovach, Caldaro-Baird, and Wynne, 2001). This report presents a structural and stratigraphic interpretation of 72 square miles (subsurface coverage) of seismic data that was reprocessed using the spectral decomposition technique. This technique detected the western limit of the upper Almond marine sand bodies and also areas saturated with hydrocarbons. The spectral decomposition method can be a valuable aid in mapping thin tight gas sands in the Rocky Mountain region.

Geological Setting

The study area lies on the Sandy Bend Arch, a southeasterly trending intra-basinal anticline in the Green River Basin between the Moxa Arch and Rock Springs Uplift (**Figure 1**). (*Note about figures: Township and range information was not labeled on field-scale figures because of the proprietary nature of WesternGeco's 3-D seismic data.*) The Green River Basin is one of the major natural gas producers in North America. The majority of its gas reserves occur in the low-permeability formations of the Cretaceous sedimentary strata. The most common Cretaceous stratigraphic units throughout the basin are the Lance Formation, Fox Hills Sandstone, Lewis Shale, Mesaverde Group (including the Almond Formation), Hilliard Shale, Frontier Formation, Mowry Shale, and Dakota Sandstone (named from top to stratigraphic base). The Almond sandstones of the Mesaverde Group are among the major gas reservoirs in southwestern Wyoming (**Figure 2**). The succession of strata comprising the Cretaceous period can be as much as 10,000 feet thick and is composed mostly of thick marine shale with multiple interbedded thin clastic layers of sandstones and siltstones. The Tertiary Fort Union Formation unconformably overlies the Lance at Stagecoach Draw Field. The pre-Cretaceous strata are poorly investigated due to a lack of wells in the study area.

The Stagecoach Draw Field, positioned approximately in the middle of the study area, produces gas from the uppermost unit of the Almond Formation, a marine

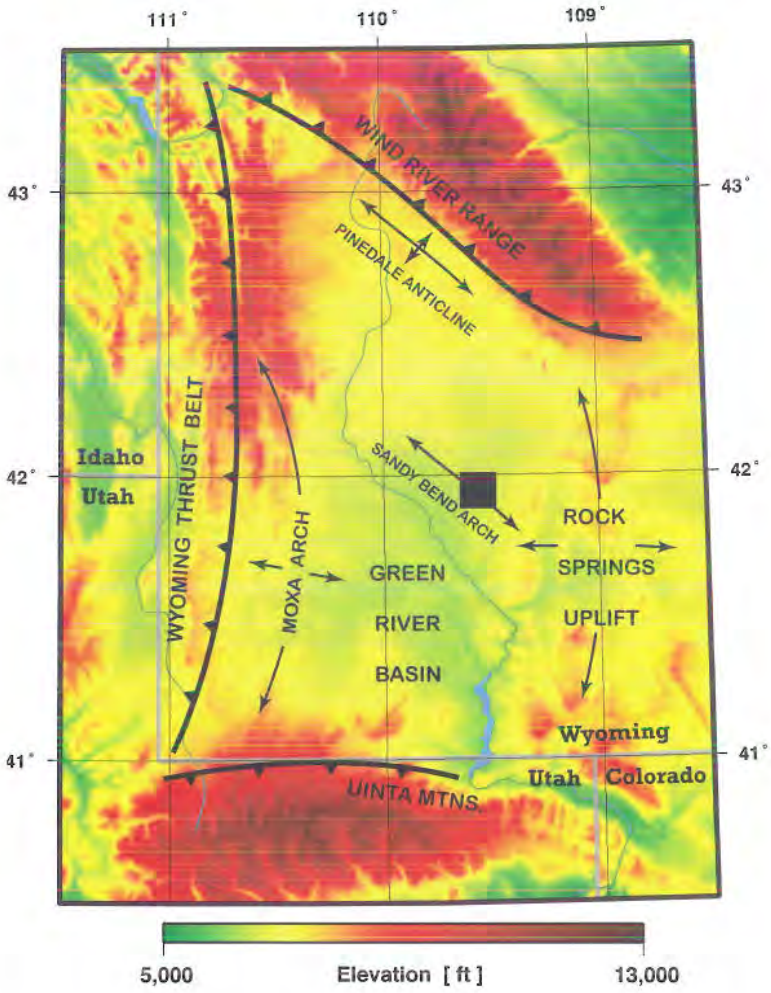

Figure 1. Location of the 3-D study area (black square) within the Green River Basin and surrounding structural elements. The map is color-coded with elevations above mean sea level. *Illustration by Yuriy Ganshin, WSGS.*

bar deposit that thins (**Figure 3**) and changes facies into lagoonal and coastal plain deposits updip and west of the field (Van Horn, 1979; Kovach, Caldaro-Baird, and Wynne, 2001). The Almond Formation at Stagecoach Draw marks the western limit of the Lewis Sea transgression (Kovach, Caldaro-Baird, and Wynne, 2001). The Almond overlies the Ericson Sandstone, a fluvially dominated clastic sediment. Two wells at Stagecoach Draw are producing from the Ericson Sandstone: Stagecoach Draw Unit 13 and 25 (Kovach, Caldaro-Baird, and Wynne, 2001; Wyoming Oil and Gas Conservation Commission, 2009). The Almond Formation at Stagecoach Draw Field is overlain by the Lance Formation (Berry, 1960).

Previous structural mapping and technical studies have established the trapping mechanism for the field, which is due to both stratigraphic segmentation and structure of variable sandstone geometries. The upper Almond marine sandstone is as much as 48 feet thick in the eastern part of the field and pinches out to the west. The subsurface has a flat-layered structure, with gas reservoirs typically at a depth of approximately 8,000 feet. Porosity and permeability from core measurements show porosity values of 12 to 17 percent for the reservoir facies and permeability values from approximately 0.01 to 50 millidarcies. Log-calculated water saturations range from 32 percent to more than 60 percent (Kovach, Caldaro-Baird, and Wynne, 2001). The field is limited in the downdip direction by a gradational gas/water contact characterized by higher average water saturation and mobile water.

The subsurface structure and tectonic setting at Stagecoach Draw play an important role in production rate. The previous seismic data analysis revealed a high-angle fault that originates from the crystalline basement and propagates upward through the

Figure 2. Upper Almond outcrop on the Rock Springs Uplift. The outcrop includes white upper shoreface sandstones over lower shoreface sandstones in the upper Almond Formation. The Almond sandstones are among the major gas reservoirs in southwestern Wyoming. *Photo by Alan J. Ver Ploeg, WSGS.*

Paleozoic section to the Dakota Sandstone horizon. The key structural element within the study area, however, is the northwest- to southeast-trending graben along the crest of the arch. En echelon normal faults that form this graben cut strata from the Fort Union Formation downward into the Hilliard Shale, with vertical displacements of as much as 170 feet in the west that decrease to the east (Kovach, Caldaro-Baird, and Wynne, 2001). The area to the south of the graben contains the best-producing wells; the area to the northeast exhibits less favorable reservoir characteristics due to a wetter reservoir phase.

Seismic and Log Data

The Big Sandy 3-D survey, approximately 72 square miles of subsurface coverage, was acquired in 1996 using the Vibroseis method. The 3-D data were reprocessed in 2008 by WesternGeco (http://www.westerngeco.com/), a business unit of Schlumberger, to produce time-migrated common-mid-point gathers and migrated stacked-amplitude volumes. The goal of reprocessing was maximum noise attenuation in the time range of 1.0 to 3.0 seconds (approximately Cretaceous-age strata) while preserving the original bandwidth. The general bandwidth of the processed data ranges from 10 to 90 hertz (Hz), which enables reliable frequency-dependent analysis.

Well logs acquired in the study area are mostly limited to approximately 8,000 feet of penetration depth to the top of the Almond Formation. The only deep well in the field, the Federal Sandy Bend No. 1 well, was drilled to a total depth of 16,413 feet and penetrated the entire Cretaceous section. Bulk density and sonic P-wave velocity logs from this well were used to calculate a synthetic seismogram by convolution

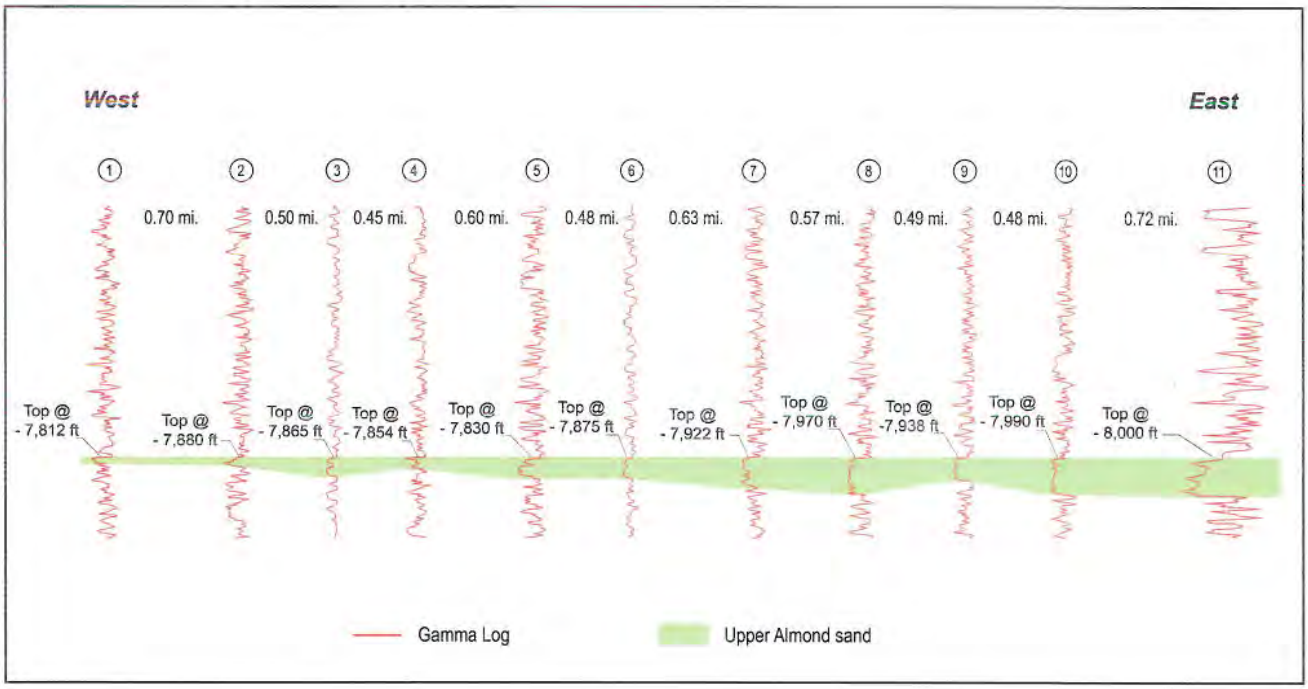

	API #	Well name	Elevation (ft)	Well total depth (ft)	Location T.	R.	sec.	Upper Almond sand thickness (ft)
①	49-037-24206	Stagecoach Draw 29	6,429	7,985	23	108	25	10
②	49-037-24086	Stagecoach Draw 21A	6,482	8,095	23	108	36	11
③	49-037-24026	Stagecoach Draw Unit 20	6,484	8,060	23	107	30	23
④	49-037-24309	Stagecoach Draw 23A	6,516	8,040	23	107	31	16
⑤	49-037-24327	Stagecoach Draw Unit 26A	6,474	8,040	23	107	30	26
⑥	49-037-23855	Stagecoach Draw Unit 7	6,492	8,074	23	107	30	28
⑦	49-037-24245	Stagecoach Draw 14A	6,481	8,130	23	107	32	38
⑧	49-037-24246	Stagecoach Draw 16A	6,523	8,150	23	107	32	46
⑨	49-037-23151	Stagecoach Draw Unit 1	6,512	8,715	23	107	32	29
⑩	49-037-24308	Stagecoach Draw 34	6,549	10,629	23	107	33	45
⑪	49-037-23857	Stagecoach Draw 9	6,541	8,130	23	107	33	48

Figure 3. West-to-east well correlation of the upper Almond sand through the Stagecoach Draw Field, using the upper Almond as a datum. This demonstrates the geometry of the Almond wedge. *Illustration by James R. Rodgers and Scott A. Quillinan, WSGS.*

with a 400-foot-long Ricker wavelet. This enabled a seismic response evaluation in the depth range from approximately 5,000 feet (lower Fort Union Formation) to approximately 16,400 feet (Morrison Formation). The depth-derived seismic response was further converted to time using the time-depth relation calculated from the velocity. The resultant, time-dependent synthetic seismogram was compared to a northeast–southwest seismic section crossing the well location and extracted from the 3-D volume.

The match between actual and synthetic data is nearly perfect, which allows unambiguous calibration of seismic horizons with stratigraphic interfaces (**Figure 4**). Similar seismic-well calibration (although within a smaller interval) was also performed with available impedance logs at two other well locations. The results of these comparisons assured fidelity of the seismic horizon interpretation completed for the Federal Sandy Bend No. 1 well. **Figure 5** shows another northeast–southwest section extracted from the 3-D seismic amplitude volume across Stagecoach Draw Field with interpreted seismic horizons. One of the field's best-producing wells, Stagecoach Draw Unit 7, appears to be drilled just south of the keystone graben (**Figure 5**). The basement-involved fault that is likely responsible for the Sandy Band Arch can be traced through the lowermost part of the sedimentary section and gradually dies out somewhere in the Hilliard Shale.

Temporal horizon mapping was performed for some major stratigraphic interfaces to clarify the structural subsurface configuration. The resulting three color-coded structure maps are shown in **Figure 6**. Seismic horizon picking along the Fort Union coals (see **Figure 4** for reference) resulted in the map shown in **Figure 6a**. The graben-bounding faults are most distinct at this stratigraphic level. There is a pronounced southwesterly dip at the basal Fort Union coals, but the dip at the Almond horizon changes to the northeast (**Figure 6b**). This indicates an angular unconformity separating Tertiary and Cretaceous deposits. The Sandy Bend Arch is not as pronounced along the Almond as it is at the Dakota horizon (**Figure 6c**). The Sandy Bend Arch hinge line is interpreted in this figure based on structure contours; however, the arch's axis bifurcates with another hinge line trending in the same northwest–southeast direction just south of the main axis (**Figure 6c**).

The Stagecoach Draw Field is in proximity to the axial surface of the Sandy Bend Arch. The keystone graben is another primary structure that controls fluid migration pathways at the reservoir level. The thickness of the upper Almond sand was determined from gamma ray logs (**Figure 3**). These data were used to construct an isopach map of the upper Almond sands (**Figure 7a**). The thickness of hydrocarbon-bearing marine Almond sandstones averages 40 feet in the Stagecoach Draw Field. This 40-foot sandy bar is embedded within shales. The Almond sand is thickest (approximately 45 feet) on the eastern margin of the study area and thins to the west to 8 feet. There are no wells drilled farther to the west to track the pinch-out. This is also the western limit of commercial production (Kovach, Caldaro-Baird, and Wynne, 2001).

The isopach map is limited to the portions of the study area that have been drilled, but well density diminishes outside of the Stagecoach Draw Field. Isopachs created through well log data are accurate for areas that have high well density but are problematic when moving into previously unexplored areas. A log data isopach map is used in this study to demonstrate the accuracy of the spectral decomposition method. Based on a visual correlation between the log-derived isopach map and mean frequency distribution (**Figure 7b**), the Almond Formation thickness throughout the entire survey can be estimated.

The interval velocities, density, and impedance corresponding to shales and productive sandstones are shown in **Table 1**. The productive sands have markedly lower impedances when compared to shales, making them good seismic reflectors. The dominant reflected signal frequencies range from 15 to 65 Hz. Thus, for an average velocity of 13,500 feet per second, the reflected wavelength (λ) range is 200 to 900 feet. The 400-foot wavelength value was used in this study to produce the synthetic seismogram in **Figure 4**.

METHOD

One of the most fundamental reservoir characteristics is thickness; however, conventional seismic data cannot resolve thin beds. Below a thickness of one quarter of a wavelength ($\lambda/4$), the top and base of a thin bed cannot be interpreted accurately (Sheriff

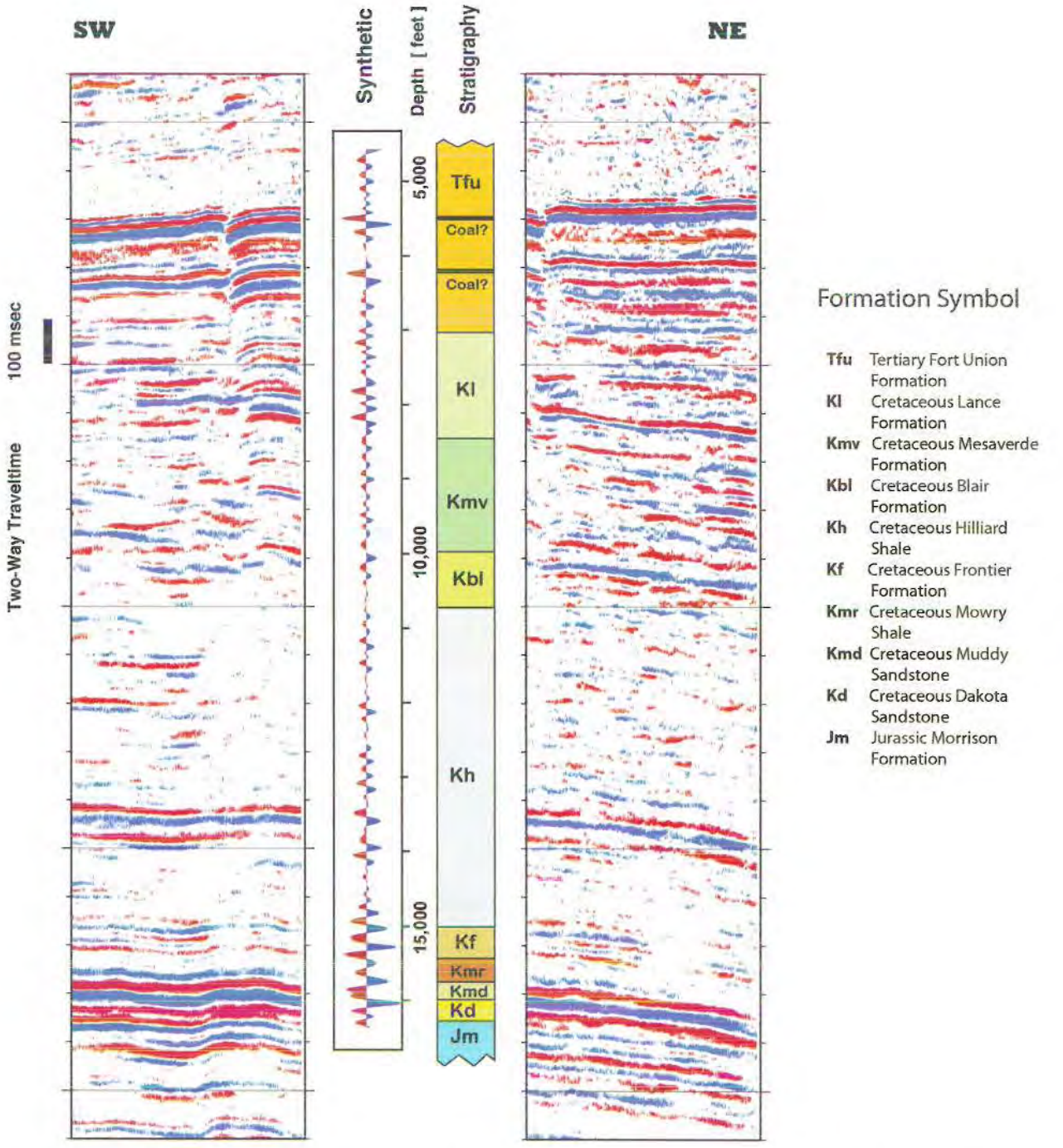

Figure 4. Northeast–southwest section from the 3-D seismic amplitude volume through the Federal Sandy Bend No. 1 well with inserted synthetic seismogram (log data convolved with 50-Hz Ricker wavelet) and stratigraphic interpretation at the well's location. *Illustration by Ganshin.*

Table 1. Geophysical properties

Lithology	Velocity (Kft/s)	Density (g/cc)	Impedance (Kft/s * g/cc)	Resistivity (ohm * m)
Sandstone	13.2	2.4	32.0	30
Shale	14.2	2.6	37.0	10

Table 1: Log-derived rock properties averaged for the Almond stratigraphic interval at Stagecoach Draw Field.

and Geldart, 1995). For a 400-foot wavelength – typical in this study – the limit of vertical resolution is approximately 100 feet. Thus, a 40-foot thick Almond bar cannot be resolved in seismic amplitudes; however, using the spectral decomposition technique reveals details unattainable through conventional seismic processing.

Spectral decomposition has emerged recently as a seismic attribute capable of producing informative images of thin beds, especially if they are stacked in sequences with sharp impedance contrasts. For example, spectral decomposition has been used for a variety of applications including layer thickness determination (Partyka, Gridley, and Lopez, 1999), stratigraphic visualization (Marfurt and Kirlin, 2001), and direct hydrocarbon detection and differentiation of fluids in a reservoir (Castagna, Sun, and Siegfried, 2003; Sinha et al., 2005). The spectral decomposition method produces a continuous time-frequency analysis of a seismic trace – that is to say, a frequency spectrum is an output for each time sample of the seismic trace. Thus, the spectral decomposition of seismic data is the process that transforms seismic amplitudes to *spectral amplitudes*, which depends not only on space and time but also on frequency. By transforming seismic data into the frequency domain, it becomes possible to relate spectral amplitude changes to thin-bed thickness variations due to preferential illumination at the "tuning" frequency (Partyka, Gridley, and Lopez, 1999). Amplitude tuning is based on the concept that reflections from a thin bed have a characteristic expression in a particular frequency band that is indicative of temporal bed thickness. In other words, higher frequencies image thinner beds, while lower frequencies image thicker beds up to approximately 100 feet in thickness.

To use horizon-based analysis, seismic horizons must be interpreted to create temporal structure maps like those shown in **Figure 6**. The seismic horizons in this study were picked manually along every five lines in the north–south and east–west directions. Horizon picks were further interpolated and smoothed with a 10x10 lines operator. Some minor picking errors may exist because of sudden wavelet changes due to faulting or stratigraphic pinch-outs. The resulting temporal structure map defines a window of data around the reservoir (or any other event of interest) that can be transformed into the frequency domain to produce a series of spectral amplitude maps at different frequencies. The so-called "tuning cube" (i.e., seismic data volume where frequency is represented by the z-direction) typically shows the amplitude of the seismic data at 1-Hz increments. The bandwidth of the seismic data (typically up to 60 Hz for the deeper horizons) limits the frequency range of the tuning cubes. This frequency volume allows the interpreter to scan through isofrequency (common frequency) images at a particular horizon, which provides snapshots of subtle changes in reservoir characteristics.

Bed thickness and stratigraphy (i.e., reflectivity series) are not the only factors that control the spectral decomposition response. Fluid type and selective attenuation of seismic waves passing through the reservoir are other key factors. A wide range of evidence suggests that hydrocarbon zones are associated with abnormally high values of seismic attenuation. In addition, abnormally high attenuation can be produced as a result of gas saturation, which also creates a velocity dispersion anomaly with reflection coefficients strongly dependent on frequency.

Wedge Modeling

A generic geologic model was constructed to explicitly examine the physical basis for links between the

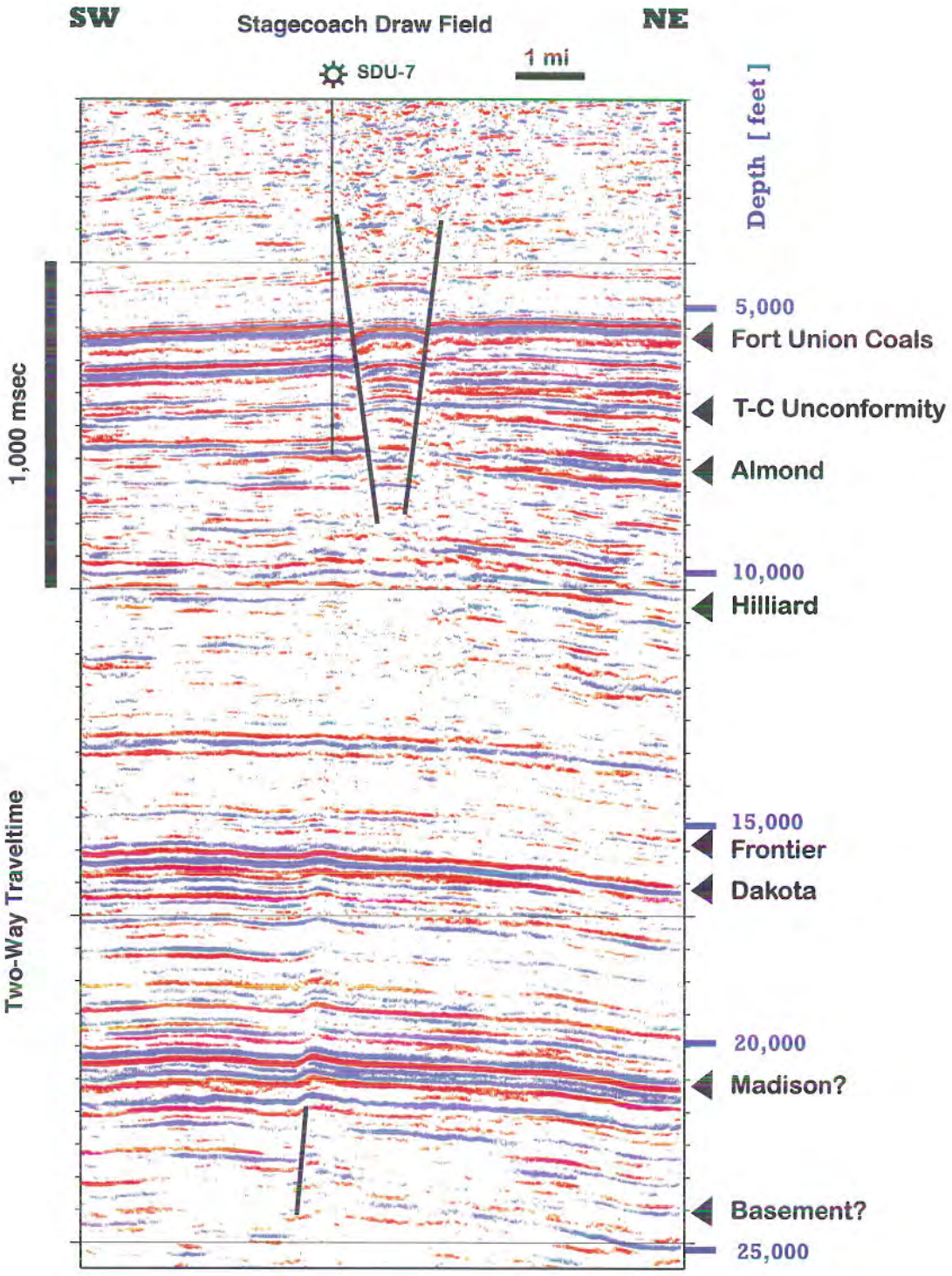

Figure 5. Northeast–southwest section from the 3-D seismic amplitude volume across Stagecoach Draw Field, through Stagecoach Draw Unit 7 well. Key stratigraphic horizons are shown on the right-hand side of the section. Major interpreted faults are shown with black solid lines. Note that the depth scale (blue notation) is nonlinear due to seismic velocity variation with depth. *Illustration by Ganshin.*

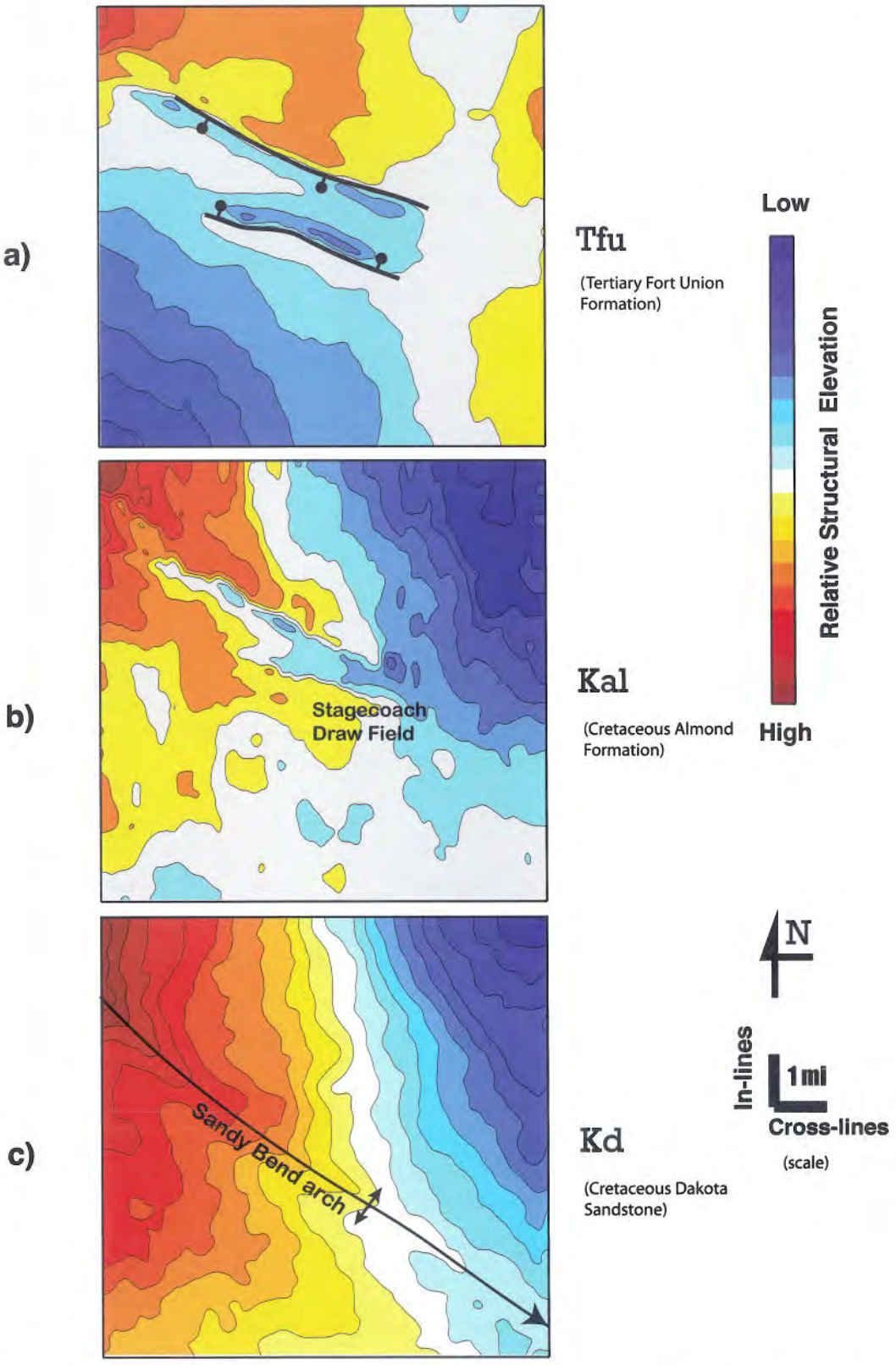

Figure 6. Temporal structure maps color-coded with relative elevation. (a) Lower Fort Union seismic horizon, (b) upper Almond seismic horizon, (c) Dakota seismic horizon. *Illustration by Ganshin.*

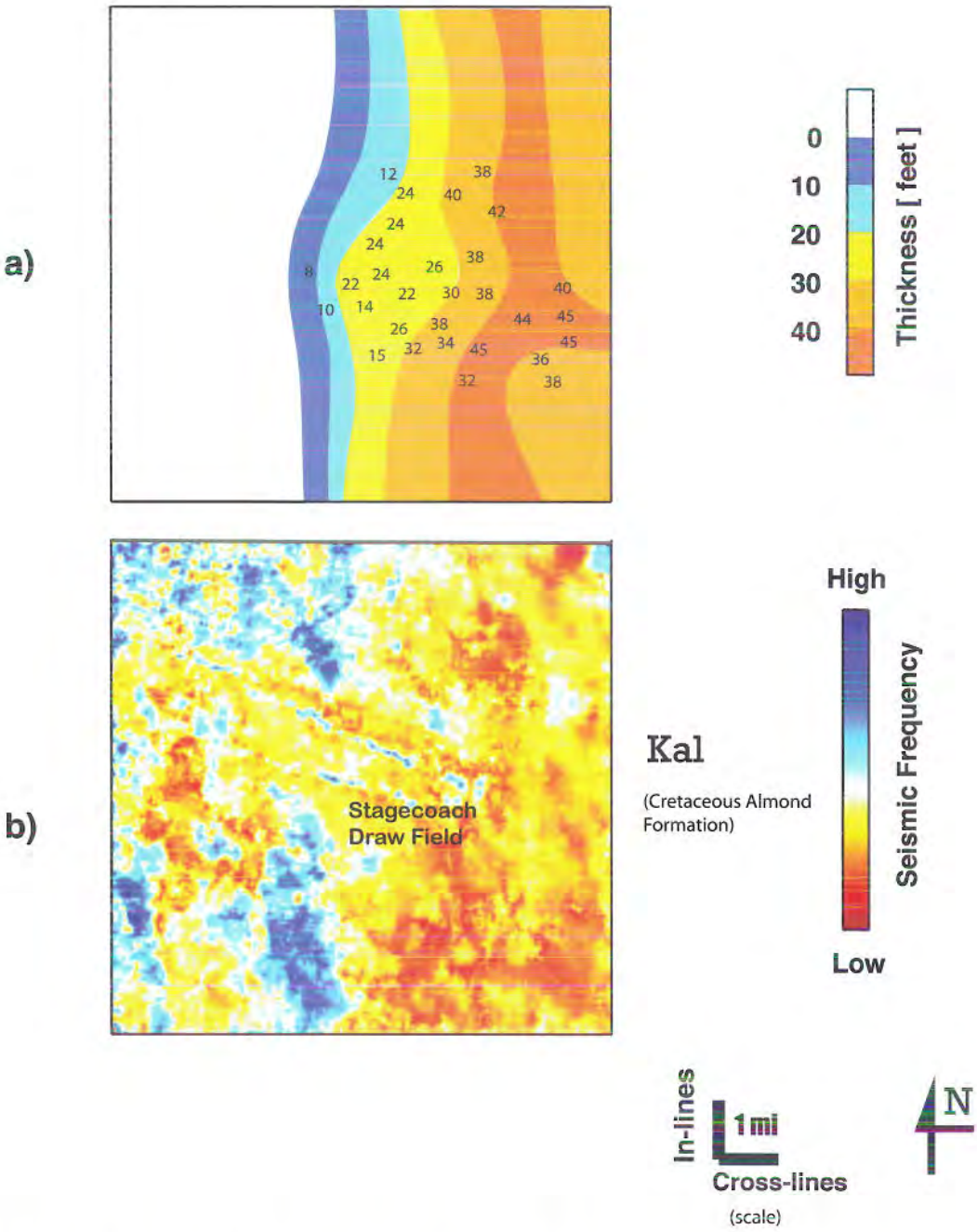

Figure 7. (a) Isopach map of the upper Almond unit. (b) Seismic frequency (weighted mean spectral value) calculated for the upper Almond seismic horizon. *Illustration by Ganshin.*

changing thickness of the wedge model and different seismic attribute responses. The density and velocity values used in the modeling are loosely based on physical properties of the Almond reservoir rocks encased in acoustically dissimilar shale (**Figure 8a**). The top and bottom of the wedge show opposite reflection polarities, which is a realistic and typical situation in most stratigraphic profiles. It was assumed that the gas-saturated sandstone wedge is lower in acoustic impedance (product of density and acoustic velocity) than the surrounding material (shale) to mimic the petrophysical profile of the Green River Basin. Correspondingly, the reflection coefficients calculated from the impedance profile

are negative at the top and positive at the bottom but with the same magnitude. The wedge thickens from a zero value on the left to 250 feet on the right, which corresponds to 50 milliseconds (msec) in two-way traveltime (**Figure 8b**).

The geologic model was convolved with the zero-phase Ormsby wavelet (limited by 4-, 8-, 60-, and 88-Hz cutoff frequencies) to produce a simple, zero-offset acoustic model of seismic response of the wedge. For a given modeling value of sandstone velocity (10,000 feet per second) and a 40-Hz average Ormsby wavelet frequency, the dominant seismic wavelength (λ) is 250 feet, which is close to the lower limit of reflection wavelength recorded at the Stagecoach Draw Field. The lateral dimension of the wedge in units of the dominant wavelength of the illuminating wavelet is marked on the top of the synthetic seismic section (**Figure 8b**). Based on the vertical resolution limit ($\lambda/4$), the model covers a thickness range from seismically thin beds ($<\lambda/4$) to intermediate ($\lambda/4 - 3\lambda/4$) and seismically thick ($>3\lambda/4$). The polarity convention of the zero-phase data adopted in this study is that a decrease in acoustic impedance is displayed as a trough filled with red color. In the zero-phase model, the seismic response to a thin bed is a trough-then-peak couplet. Therefore, the top of sandstone corresponds to a main seismic trough (red fill in **Figure 8b**), whereas the base of the sandstone bed can be correlated to a main seismic peak (blue fill in **Figure 8b**).

Figure 8b shows antisymmetric waveforms that correspond to the top and bottom of the sandstone having variable thickness. For seismically thin and intermediate beds, reflection amplitudes are composite seismic responses resulting from interference of the top and the bottom reflections.

In **Figure 9a**, seismic signal variability is examined along the upper shale-sandstone interface that is marked with black squares over the red troughs. When the sandstone bed thins to below $\lambda/4$, a time deviation between the horizontal reflection interface and maximum seismic energy (trough) occurs. This phenomenon makes it difficult to measure accurate times along the top and base reflectors. The tuning thickness is manifested seismically by increased amplitude – the effect called *tuning* is a response to a constructive interference of the reflections from the top and base of the thin bed (Sheriff and Geldart, 1995). The *tuning thickness* refers to the thinnest interval over which a correct measurement of arrival times still can be made for both interfaces. Tuning is important for hydrocarbon reservoir characterization and other thin-bed interpretation situations.

The reservoir bodies in the Green River Basin are often thinner than the tuning thickness, and therefore a special approach, other than conventional amplitude measurement, is required to determine reservoir thickness variations. In this study, the spectral decomposition technique was used to describe changes in spectral behavior along the top shale-sandstone interface. This concept illustrates that a reflection from a thin bed has a characteristic expression in the frequency domain.

The amplitude and frequency tuning curves measured from the seismic response are shown in **Figures 9b** and **9c**, respectively. Horizontal axes of these curves are labeled in the dominant wavelength to indicate the thickness of the wedge. The amplitude tuning curve is characterized by two maxima at approximately $\lambda/5$ (50 feet) and $\lambda/2$ (125 feet). These maxima occur when the central trough of the top reflection interferes positively with the side lobe of the wavelet from the bottom interface. As the wedge thins to less than $\lambda/5$, the amplitude starts to vanish continuously. Although the nonlinear changes in seismic amplitude are the well-established effects of thin-bed tuning, the corresponding changes in seismic signal frequency are much less documented. The authors attempted to fill this gap by calculating mean frequency of spectrally decomposed reflection that corresponds to the top of the wedge.

Figure 9c shows the frequency effect of convolving reflections and side lobes from the upper and lower interfaces that are variably aligned. The effect is similar to the way in which the seismic frequency content is degraded during the stacking process of imperfectly aligned primary reflections. The frequency-tuning curve demonstrates a general oscillating behavior around an average wavelet's frequency of 40 Hz. The most important changes in frequency occur from zero to $\lambda/3$ (approximately 85 feet for the model parameters) when the wedge thickens. There is also a large corresponding decrease in frequency (approximately 20

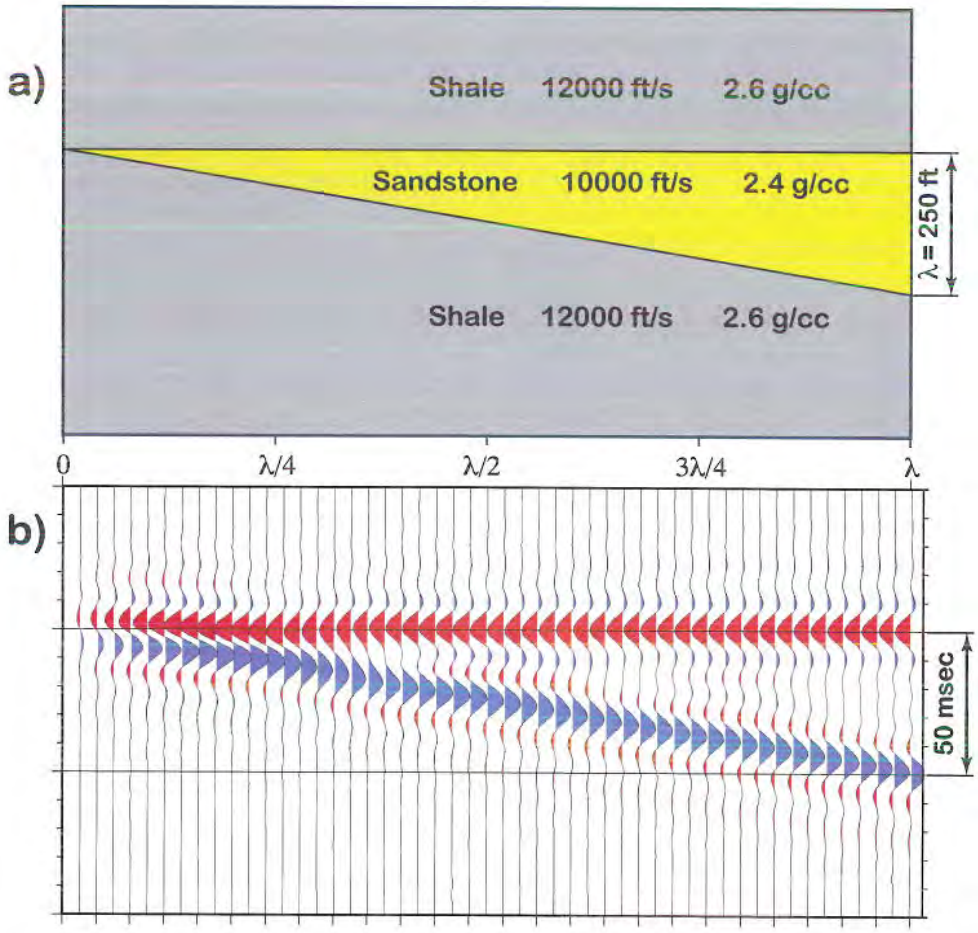

Figure 8. (a) Geometry of the wedge model, approximating sandstone layer encased in thick shale. (b) Seismic response generated using zero-phase Ormsby wavelet with the four corner frequencies 4, 8, 60, and 88 Hz. The thickness of the wedge in units of the dominant wavelength (λ) of the Ormsby wavelet is marked along the top of the seismic section. *Illustration by Ganshin.*

Hz), which is approximately 50 percent of the modeled wavelet's average frequency (**Figure 9c**). The inversely proportional behavior of the frequency-tuning curve for beds with thickness below λ/3 is utilized in this study. It should be noted that the majority of siliciclastic reservoir rocks in the Green River Basin measure 5 to 100 feet in thickness, which is below one-third of a dominant seismic wavelength. Therefore, time-frequency analysis should become an essential part of seismic data processing for reservoir characterization.

Figures 10a and **10b** show spectral amplitude profiles for the same wedge model as **Figure 8a**. The profiles were generated as common frequency images for 30 Hz and 60 Hz that show a relative difference in amplitude at different frequencies. A comparison of relative spectral amplitude distribution clearly indicates that the amplitude peak moves toward the thinner part of the wedge with increasing frequency (**Figure 10**). The relative spatial propagation of amplitude peak with changing spectral frequency is another important property of the wedge model utilized in this study.

The inversely proportional dependence of seismic frequency on thickness for beds thinner than one third of dominant seismic wavelength is not a result of specific modeling parameters. The authors tested wedge models with both positive and negative impedance contrasts of the embedded layer. The authors also analyzed frequency response of the wedge model produced by 90°-phase wavelets with different average frequencies. The modeling results indicate that, in all

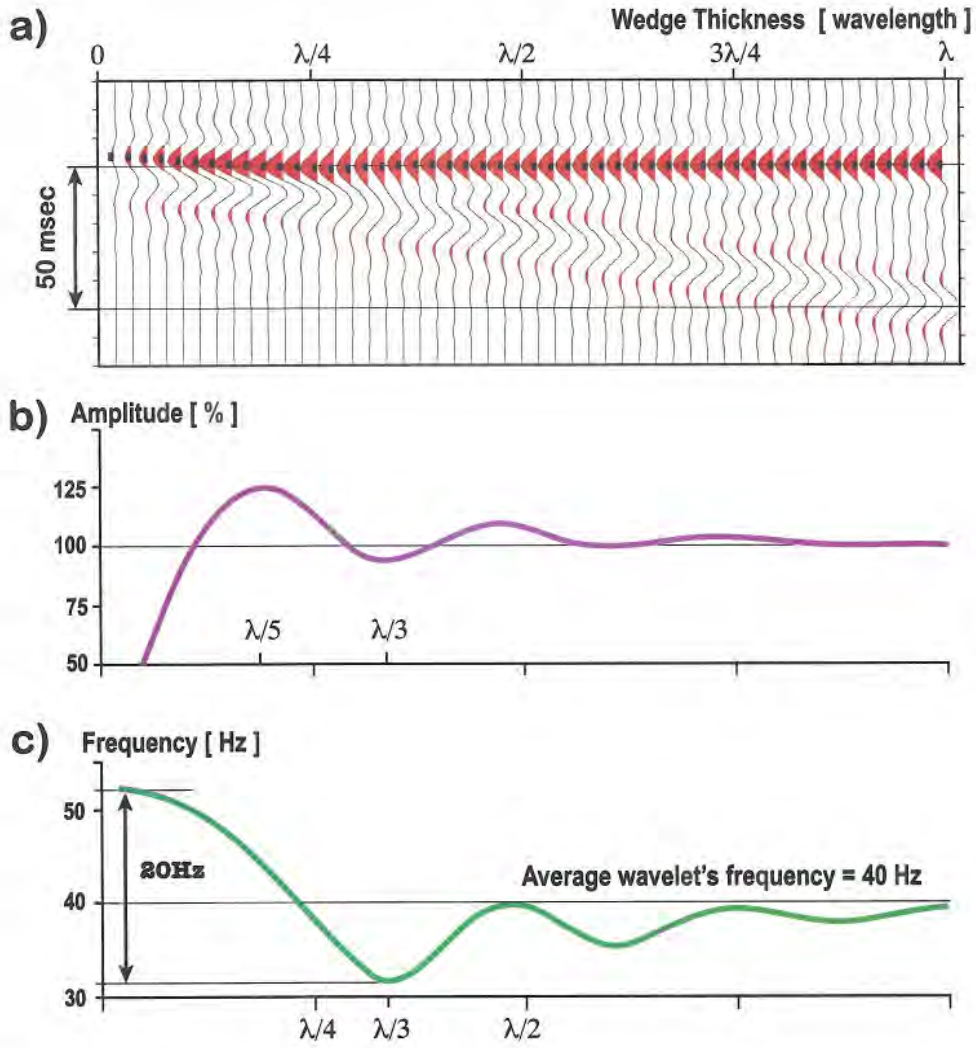

Figure 9. (a) Wedge seismic response generated using zero-phase Ormsby wavelet with the four corner frequencies 4, 8, 60, and 88 Hz. Black ticks are the top of the wedge tracked by the central trough location. (b) Amplitude and (c) peak frequency variations at the top of the wedge model. *Illustration by Ganshin.*

cases, the lowest measured frequency corresponds to the wedge thickness equivalent to λ/3. Note that this frequency "tuning" matches to the bed thickness that is measured in relative units of seismic wavelength.

Delineation of the Almond Reservoir Sandstone

The study area encloses the Stagecoach Draw Field with a number of wells within the field that can be utilized as control points for production. The largest challenge lies in mapping prospect areas that have not been drilled and are not connected to previously discovered gas wells. Spectral decomposition was successfully used to indicate lateral heterogeneity of the upper Almond marine sandy bar. **Figure 11** shows two isofrequency panels with the reservoir indicated. These vertical sections were extracted from the spectrally decomposed seismic data volume. The selection was done in the northeast–southwest direction (across the Sandy Bend Arch) through the Stagecoach Draw Unit 7 well. A strong spectral amplitude tuning effect can be observed in the northeast on the 20-Hz panel at the

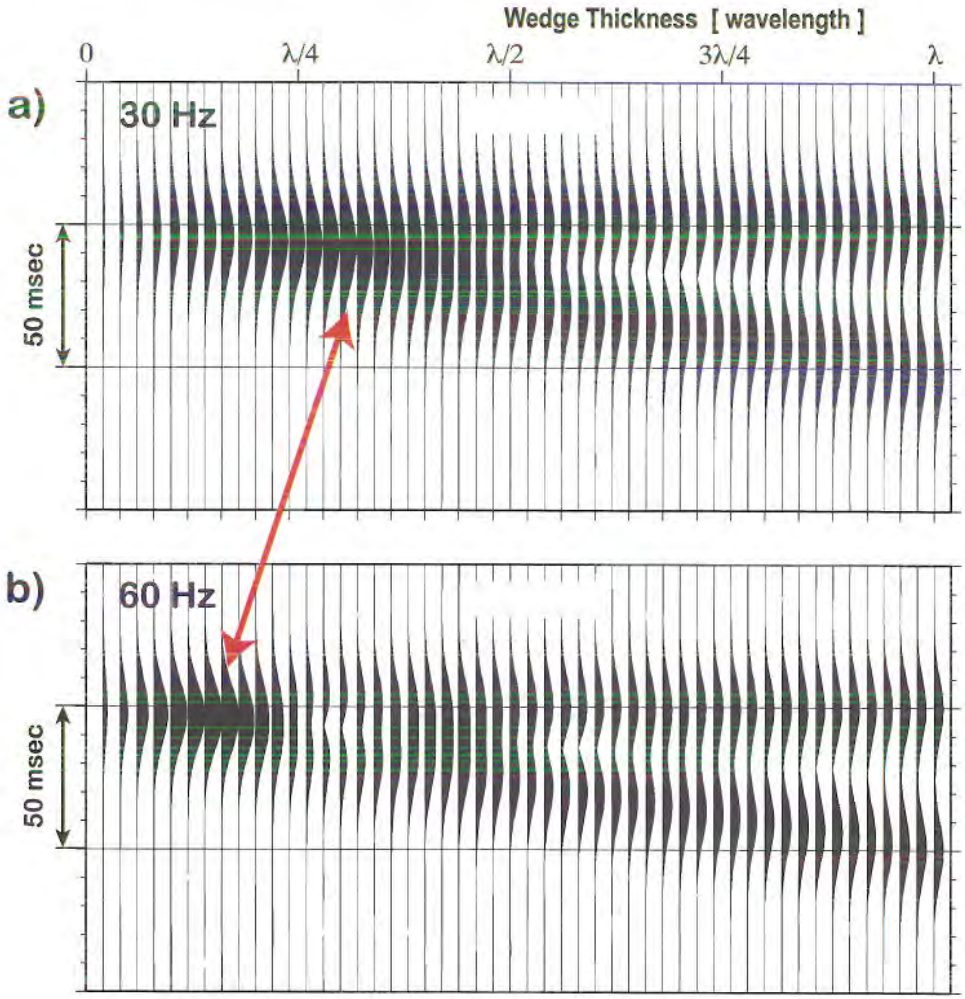

Figure 10. Spectral amplitude profiles for the seismic wedge model. (a) 30-Hz and (b) 60-Hz common frequency images. Note that the amplitude peak moves toward the thinner part of the wedge with increasing frequency. *Illustration by Ganshin.*

reservoir level, which is indicated with the "Almond" icons in **Figure 11**. This behavior can be explained by the fact that the time-thickness of the northeasterly deposited Almond bar is close to tuning. The Almond bar thins out westward and can be imaged through the whole panel only at higher frequencies (25-Hz panel in **Figure 11**).

Figures 12a–12c show three isofrequency images selected from the Almond "tuning cube" (i.e., the spectral amplitude maps obtained along the Almond stratigraphic interval for three different common frequency values). The 15-Hz common frequency image illuminates the thickest Almond deposits with high amplitudes (red-color areas in **Figure 12a**). Destructive thin bed interference causes notches and general amplitude decay in the 20-Hz common frequency image (**Figure 12b**). Finally, the 25-Hz isofrequency image for the same horizon highlights the thinnest areas of the Almond reservoir sandstone development. The westernmost reservoir dimensions are outlined by the dashed contour in **Figures 12b–12c**. The isofrequency displays in **Figure 12** show anomalies having distinct patterns. These anomalies, when integrated with well data, suggest the depositional geometries of the productive sandstones. When animating through the whole range of frequencies of the Almond "tuning cube," it can be easily observed how the amplitude peak moves toward the thinner part of the wedge with increasing frequencies. Viewing amplitude-dependent effects in map view is also revealing. For example, the north-

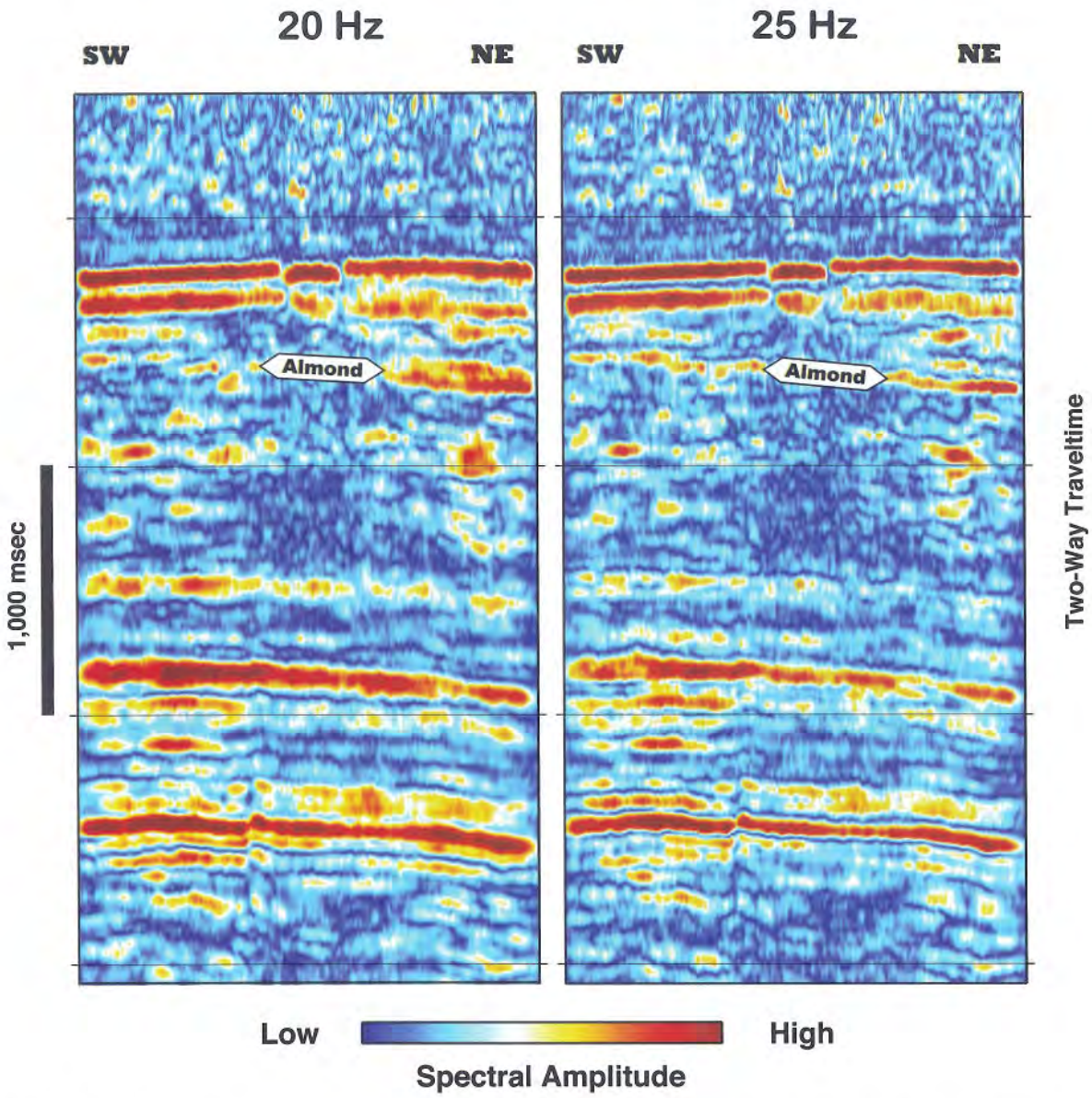

Figure 11. Northeast–southwest isofrequency sections from the spectrally decomposed 3-D seismic volume across Stagecoach Draw Field. Note a relative amplitude increase and reflections continuity at the Almond reservoir interval (labeled area) at 25 Hz (right panel) compared to 20 Hz (left panel). *Illustration by Ganshin.*

west–southeast-trending low-amplitude fault zones can be easily tracked at all frequencies (**Figures 12a–12c**).

Figure 13 shows two sequential horizon slices selected from the 20-Hz common frequency volume. **Figure 13a** corresponds to the Almond reservoir interval (same as in **Figure 12b**). **Figure 13b** shows spectral amplitude distribution just 50 msec below the reservoir. There is pronounced amplitude "shadow" in the southeast part of the study area (**Figure 13b**). Based on this interpretation, this low amplitude, which is also present at all other frequencies, is evidence of the attenuation by the reservoir of seismic waves passing through the gas column. Note that the low-amplitude area in **Figure 13b** corresponds to the high-amplitude area in **Figure 13a** and is consequently caused by gas-related attenuation. The northeast corner in both slices

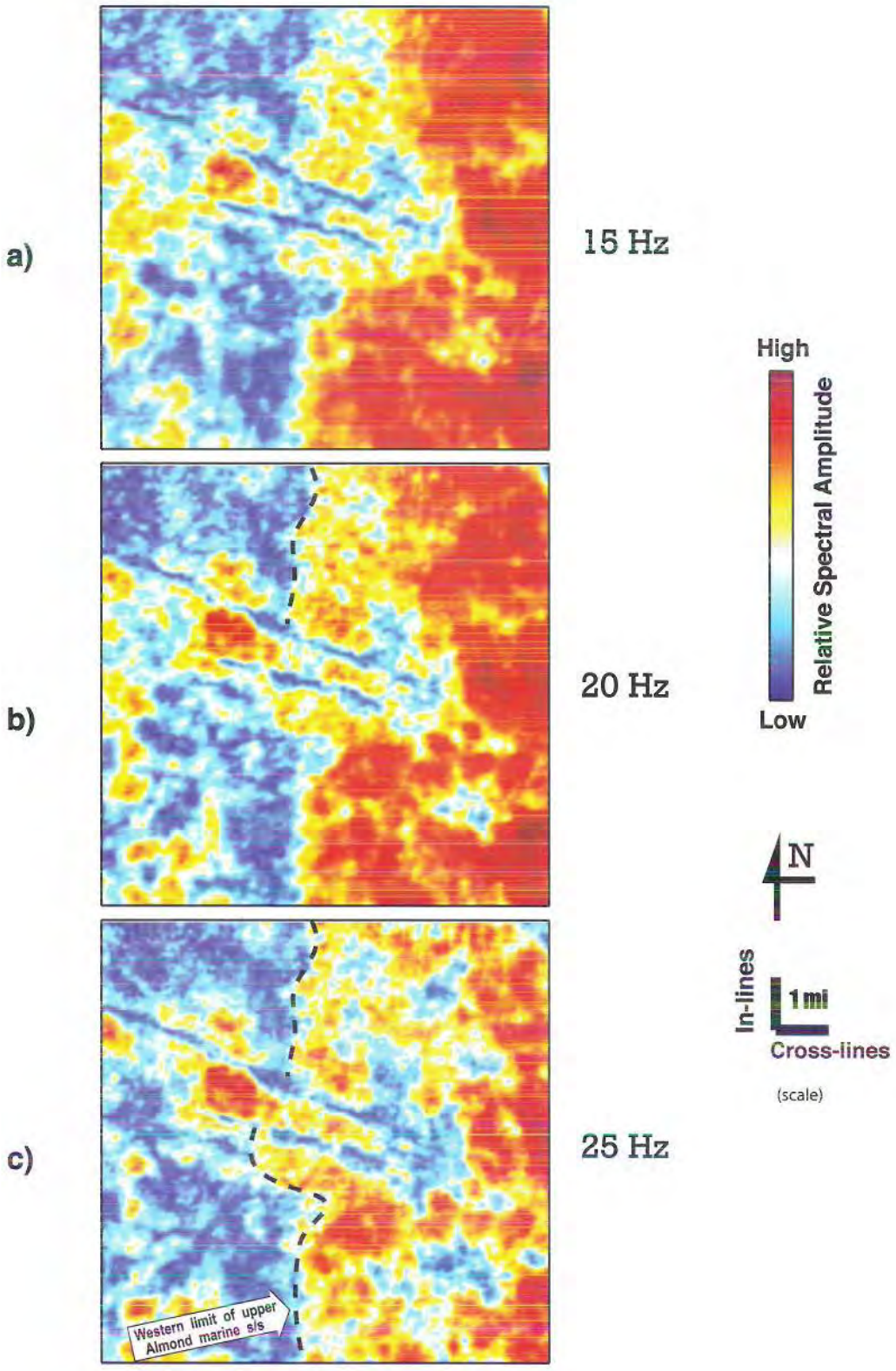

Figure 12. Spectral amplitude maps of the Almond stratigraphic interval selected from different common frequency volumes. (a) 15-Hz, (b) 20-Hz, and (c) 25-Hz common frequency images. Note that the high-amplitude Almond horizon (red colors) progressively thins out to the west. *Illustration by Ganshin.*

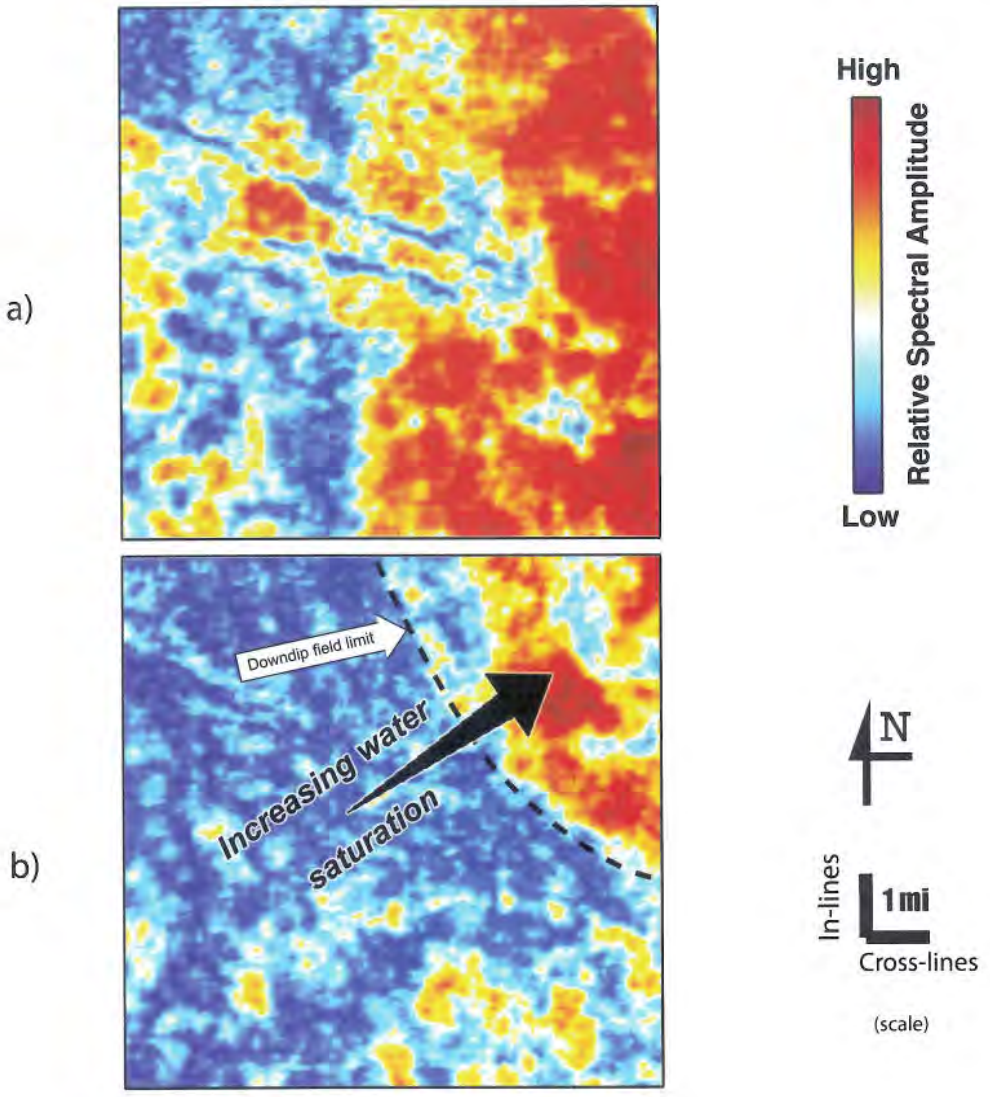

Figure 13. Map views of sequential horizon slices selected from the 20-Hz common frequency volume. (a) Spectral amplitude variations along the Almond stratigraphic interval. (b) Spectral amplitudes just 50 milliseconds below the Almond reservoir. Note that the low-amplitude shadow produced by the gas column in the southeast corner due to preferable seismic energy attenuation. *Illustration by Ganshin.*

is characterized by relatively high amplitude values that indicate absence of anomalous attenuation. This is interpreted as an area of increased water saturation and is approximately outlined by the dashed contour in **Figure 13b**.

The interpreted pay zone within the study area is outlined in **Figure 14**. The western limit of upper Almond marine sandstone and the area of increased water saturation are shown over the time-structure map of the Almond stratigraphic interval. It appears that the interpreted area of increased water saturation has a pronounced structural control. It separates the low-elevation area in the northeast (big values of two-way traveltime) from the uplifted horizon surface in the west (**Figure 14**). The westernmost limit of the pay zone is largely controlled by depositional changes (marine vs. coastal) rather than structural configuration. The red symbols in **Figure 14** represent well locations, with the circle size proportional to gas production. The Stagecoach Draw Field appears to coincide with a subtle structural high (possibly a plunging nose

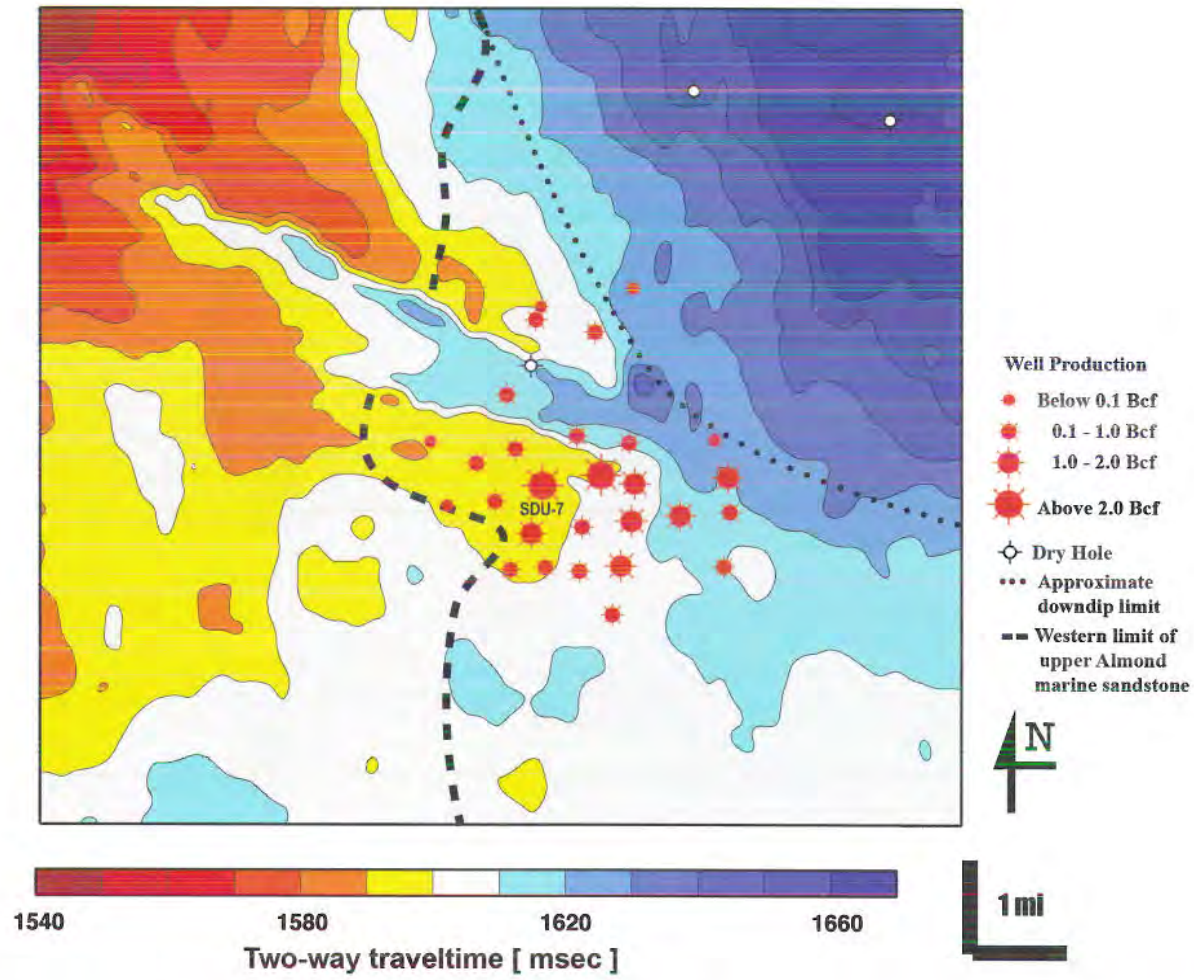

Figure 14. Time-structure map along the Almond stratigraphic interval in the study area. The western limit of the upper Almond sandstone and the downdip limit of the field are interpreted from the common frequency images. Red symbols correspond to the gas-producing wells, with the circle size proportional to the cumulative production of the wells. *Illustration by Ganshin.*

of the Sandy Bend Arch) along the Almond horizon. The key graben splits the field into two parts, with the best production established in the southern part (**Figure 14**). Natural fracturing associated with faulting along the key graben possibly determines increased Almond permeability at this location; however, there is a large unexplored territory in the southeast with good gas production potential. This potential is outlined from the seismic analysis performed in this study and shown in **Figure 14**. More evidence of gas saturation comes from Samson Oil & Gas Limited (http://www.samsonoilandgas.com/) reports on the Stagecoach East Field development. Samson has acquired acreage that is just south of the southeast corner of the study area. The nearby Stratos Federal No. 1 test well intersected approximately 20 feet of gas shows with good permeability and porosity as measured by wire-line logs within the Almond Formation (Samson Oil & Gas Limited, 2007).

Conclusions

The extent of the Almond productive sandstones has been mapped using spectral decomposition technique. Reservoir and non-reservoir facies were differentiated by a comprehensive, integrated seismic attribute analysis. The spectral decomposition method is a valuable aid in enhancing the ability to map thin beds in the tight gas sands environment of

the Rocky Mountain region. Results from this study can be integrated in the reservoir modeling and site characterization phases of the Stagecoach Draw Field development. This method also directly detected and mapped gas-saturated reservoir rocks. Therefore, the spectral decomposition method can be used as a quick indicator of gas saturation for natural gas occurrences.

Acknowledgments

The authors acknowledge WesternGeco for allowing publication of the 3-D seismic data and Mary Palen-Murphy, in particular, who did the preliminary data preparation and conditioning for frequency analysis. We thank Michael Vervalin, WesternGeco sales manager in the company's Denver, Colorado, office, and other representatives of WesternGeco who reviewed our paper. We also acknowledge GMT (http://gmt.soest.hawaii.edu/), a collection of freeware programs developed by Paul Wessel and Walter H.F. Smith. The programs facilitated the processing and plotting of scientific data. We also recognize colleagues who have worked with us on the Stagecoach Draw Field study and who supported the preparation of this paper. They include Rodney De Bruin, Wyoming State Geological Survey (WSGS) assistant director, and Fred McLaughlin, WSGS manager of regional geology, mineral, and water resources. We thank Robert Waggener, WSGS editor in chief, James Rodgers, WSGS petroleum engineer, Alan Ver Ploeg, WSGS assistant director, Tamara Linse, consulting technical editor, and Brendon Orr, consulting graphic designer, for their great efforts that made this publication possible.

References Cited

Berry, D.W., 1960, Geology and ground-water resources of the Rawlins area, Carbon County, Wyoming: U.S. Geological Survey Water-Supply Paper 1458, 1 plate, scale 1:63,360, 74 p.

Castagna, J.P., Sun, S., and Siegfried, R.W., 2003, Instantaneous spectral analysis; detection of low-frequency shallows associated with hydrocarbons: The Leading Edge, v. 22, no. 2, p. 120–127.

Kovach, P.L., Caldaro-Baird, J.L., and Wynne, P.J., 2001, Stagecoach Draw Field: Gas production from the westernmost marine-influenced deposits of the Lewis Seaway transgression into southwestern Wyoming, *in* Anderson et al., eds., Gas in the Rockies: Rocky Mountain Association of Geologists, Denver, Colorado, p. 125–144.

Marfurt, K. J., and Kirlin, R.L., 2001, Narrow-band spectral analysis and thin-bed tuning: Geophysics, v. 66, no. 4, p. 1274 –1283.

Partyka, G. A., Gridley, J.M., and Lopez, J.A., 1999, Interpretational applications of spectral decomposition in reservoir characterization: The Leading Edge, v. 18, no. 3, p. 353–360.

Samson Oil & Gas Limited, 2007, Stage Coach East #1 well spuds: Samson Oil & Gas Limited ASX Announcement: *at* http://samsonoilandgas.com/IRM/content/investor_asxannouncements.html (accessed 2007; site now discontinued).

Sheriff, R.E., and Geldart, L.P., 1995, 6.4.2 vertical resolution and 6.4.3 tuning and thin-beds effects, *in* Exploration Seismology (2nd ed.), Cambridge University Press, p. 173–174.

Sinha, S., Routh, P.S., Anno, P.D., and Castagna, J.P., 2005, Spectral decomposition of seismic data with continuous-wavelet transform: Geophysics, v. 70, no. 6, p. 19–25.

Van Horn, M.D., 1979, Stratigraphy of the Almond Formation, east-central flank of the Rock Springs Uplift, Sweetwater County, Wyoming: A mesotidal shoreline model for the late Cretaceous: M.S. thesis, Colorado School of Mines, Golden, Colorado, 179 p.

Wyoming Oil and Gas Conservation Commission, 2009, Wyoming Oil and Gas Conservation Commission: *at* http://wogcc.state.wy.us/ (accessed April 2009).

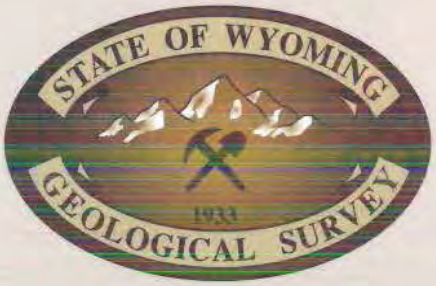

WSGS

www.wsgs.uwyo.edu

Mission Statement

The Wyoming State Geological Survey (WSGS) mission is to promote the beneficial and environmentally sound use of Wyoming's vast geologic, mineral, and energy resources while helping protect the public from geologic hazards. By providing accurate information and expanding knowledge through the application of geologic principles, the WSGS contributes to economic growth and improvement in the quality of life for Wyoming's residents.

Advisory Board Members

Ex officio

Governor Dave Freudenthal, State of Wyoming
WSGS Director and State Geologist Ronald C. Surdam
Supervisor Thomas Doll, Wyoming Oil and Gas Conservation Commission, *board vice president*
Vice President William Gern, University of Wyoming Office of Research and Economic Development

Appointed

Lisa Lindemann, Cheyenne
Chris Mullen, Casper, *board president*
John Simons, Cheyenne
John Trummel, Gillette, *board secretary*
Wallace Ulrich, Jackson

9 781884 589522